Asian Journal of Pharmaceutical Sciences 16 (2021) 86–96

Available online at www.sciencedirect.com

ScienceDirect

journal homepage: www.elsevier.com/locate/AJPS

Original Research Paper

3D printing-based drug-loaded implanted prosthesis to prevent breast cancer recurrence post-conserving surgery

Wenyan Hao[a,b,#], *Zengjuan Zheng*[b,#], *Lin Zhu*[a], *Lulu Pang*[a,c], *Jinqiu Ma*[a,c], *Siqing Zhu*[a,d], *Lina Du*[a,b,c,d,*], *Yiguang Jin*[a,d,*]

[a] *Department of Pharmaceutical Sciences, Beijing Institute of Radiation Medicine, Beijing 100850, China*
[b] *Weifang Medical University, Weifang 261000, China*
[c] *Shandong University of Traditional Chinese Medicine, Jinan 250355, China*
[d] *Anhui Medical University, Hefei 230032, China*

ARTICLE INFO

Article history:
Received 16 January 2020
Revised 25 May 2020
Accepted 15 June 2020
Available online 7 July 2020

Keywords:
Prosthesis
Breast cancer
Microspheres
Paclitaxel
Doxorubicin
Metastasis

ABSTRACT

Systemic chemotherapy of breast cancer is commonly delivered as a large dose and has toxic side effects. Local chemotherapy would overcome the shortcomings of systemic reconstruction and could play an important role in breast cancer surgery according to personalized demand. The application of three-dimensional (3D) printing technology makes personalized customization possible. We designed and prepared a prosthesis containing paclitaxel (PTX) and doxorubicin (DOX) microspheres (PPDM) based on 3D printing to prevent tumor recurrence and metastasis after breast conserving surgery. Polydimethysiloxane has good biocompatibility and was used as a drug carrier in this study. The average particle size of the PTX and DOX microspheres were approximately 3.1 μm and 2.2 μm, respectively. The drug loading of PTX and DOX microspheres was 4.2% and 2.1%, respectively. *In vitro* drug release studies demonstrated that the 3D-printed prosthesis loaded with PTX and DOX microspheres could release the drugs continuously for more than 3 weeks and thereby suppress cancer recurrence with reduced side effects. The PTX and DOX microspheres not only exerted a synergistic effect, but also achieved a good sustained release effect. *In vivo* evaluation showed that the PPDM could effectively inhibit breast cancer recurrence and metastasis in mice with breast cancer. PPDM are expected to achieve postoperative chemotherapy for breast cancer and be highly efficient to prevent local breast cancer recurrence and metastasis.

* Corresponding authors.
E-mail addresses: dulina@188.com (L.N. Du), jinyg@sina.com (Y.G. Jin).
# The two authors contributed equally to this article.
Peer review under responsibility of Shenyang Pharmaceutical University.

https://doi.org/10.1016/j.ajps.2020.06.002

1. Introduction

Breast cancer is the most common malignant tumor in women worldwide. It has a serious influence on women's life and health, and its incidence is increasing [1]. At present, breast cancer treatment includes surgical resection, radiotherapy, chemotherapy and comprehensive treatment [2]. Breast cancer is a systemic disease, and the failure of breast cancer treatment mainly results in systemic metastasis. However, for surgical resection, if the scope of surgery is expanded blindly, the survival and healing rates of patients will decrease. Breast-conserving surgery has become common because it can achieve a cure and improves patients' quality of life. In addition, breast reconstruction has become indispensable for breast cancer treatment [3,4]. The success of breast implant surgery is determined by the clinical experience of the surgeon. Currently, prostheses prepared by mass production in large quantities are usually unable to adapt to the breast anatomy of individual patients with breast cancer. Therefore, personalized prosthesis is of great significance. As a biocompatible and cost-effective human implant, silicone prostheses are safe, have good flexibility, and are widely used in medical research. 3D printing technology is an emerging manufacturing technology that brings major innovations in the biomedical field, including drug delivery. 3D printing has the advantage of accurate and rapid customization of personalized products [5,6].

For patients with breast cancer, local recurrence is the most serious problem after breast-conserving surgery. Therefore, postoperative chemotherapy is common and imperative. However, systemic chemotherapy has many disadvantages, such as large dosage, toxic effects and frequent daily administration. Chemotherapy via local sustained release implants can overcome the many shortcomings of systemic administration [7]. The main objectives of local implants are to reduce administration times, improve the compliance of patients, and maintain the controlled or sustained release of drugs [8], with the aim of killing residual tumors to prevent recurrence.

Microspheres are spheroidal particles comprising drugs and suitable polymers, which are commonly used for controlled/sustained release drug delivery systems [9]. A biodegradable triblock copolymer, poly lactic-co-glycolic acid (PLGA), is used commonly to prepare microspheres or nanoparticles for sustained or controlled drug release [10]. PLGA-polyethylene glycol-LGA (PLGA-PEG-PLGA) was developed as an injectable hydrogel containing dissolved paclitaxel, which exhibited a fairly long release period for 6 weeks [11]. Paclitaxel (PTX) and doxorubicin (DOX) are widely used for chemotherapy of various solid tumors in the clinic, with excellent antitumor effects, especially as a sequential combination to treat breast cancer [12]. Clinical studies have shown that the total effective rate of the drug combination was as high as 68%, while the effective rate of PTX alone for breast cancer patients was about 39%. The anti-cancer effect improved significantly, with decreased adverse reactions, and few allergic reactions and cardiotoxicity by the combined use of PTX and DOX [13].

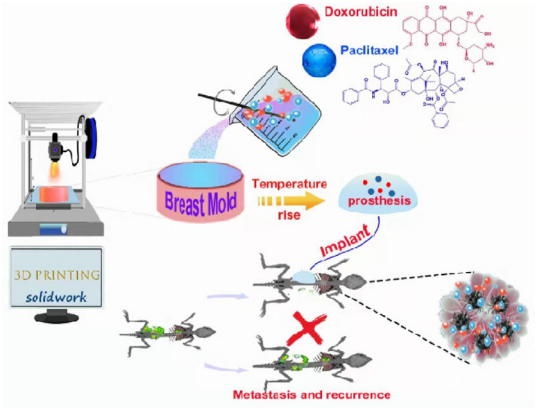

Fig. 1 – Illustration of production of a prosthesis loaded with PTX and DOX microspheres.

In the present study, a breast mold was printed based on 3D printing technology. Fig. 1 shows the concept of the design of the 3D printing-based drug-loaded implanted prosthesis for the prevention of breast cancer recurrence post-conserving surgery. A polydimethysiloxane (PDMS) prosthesis loaded with microspheres of PTX and DOX was prepared using the printed breast mold. The physiochemical properties of the prepared prosthesis was evaluated, including morphology, drug loading efficiency, encapsulation efficiency and drug release *in vitro*. Then, the therapeutic efficacy and systemic toxicity of the prosthesis was evaluated in a mouse model of local recurrence and metastasis of breast cancer. The results demonstrated that the 3D-printed prosthesis loaded with microspheres of PTX and DOX could release the drugs continuously for more than 3 weeks and suppressed cancer recurrence with reduced side effects.

2. Materials and methods

2.1. *Materials*

The chemicals and their commercial sources were as follows: DOX (Aladdin, Shanghai, China); PTX (Nanfang Pharmaceutical Co., Ltd., Fujian, China); 4′,6-diamidino-2-phenylindole (DAPI; Sigma, St. Louis, MO, USA); PLGA (LA/GA = 50/50, MW 10,000; Shandong Institute of Medical Devices, Jinan, China); Polyvinyl alcohol (PVA; Yili Fine Chemicals Co., Ltd., Beijing, China); Dichloromethane and phosphate (Sinopharm Chemical Reagent Co., Ltd., Beijing, China); Tween 80 and Tween 20 (Volkswagen Pharmaceutical Factory, Shanghai, China); Sodium lauryl sulfate (Amresco, Solon, OH, USA); Polydimethysiloxane Sylgard 184 (PDMS, viscosity at 25 °C 3500 cP; DOW CORNING Co., Ltd.,); LCD photosensitive resin (Shenyue Technology Co., Ltd., Shenzhen, China); CCK-8 (Gen-View, Scientific Inc., Jacksonville, FL, USA); Chloral hydrate was supplied by 307 Hospital of PLA. Trypsin-EDTA and Dulbecco's modified Eagle's medium (DMEM) basic were supplied by Gibco Co., Ltd.(Grand Island, NY, USA).

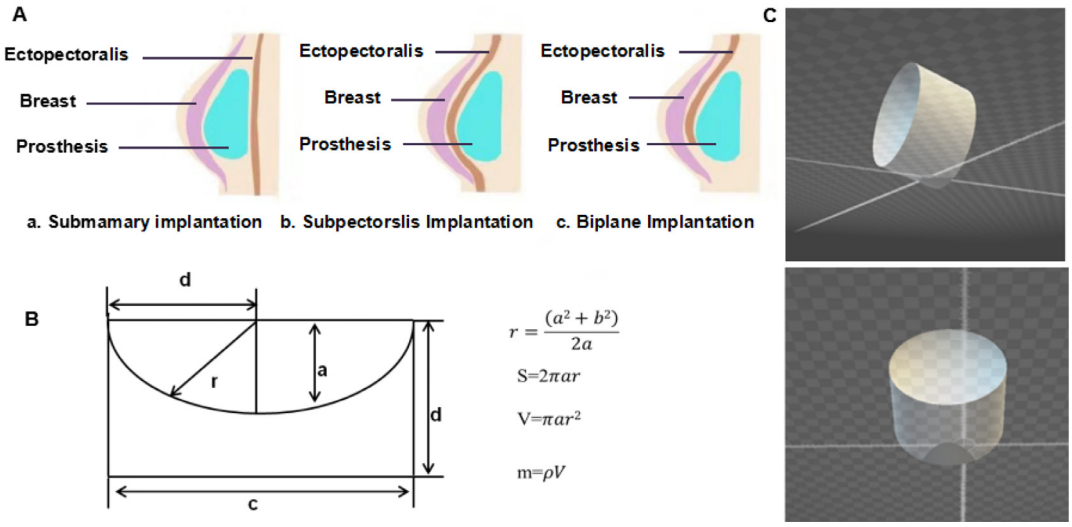

Fig. 2 – The design and 3D printing of mouse breast mold. (A) Scheme of clinical prosthesis implantation. (B) The section and calculation of prosthesis mold. (C) The design model of prosthesis mold.

2.2. *Cell lines*

Luciferase tagged 4T1 cells (4T1-luc; a mouse breast cancer cell line) were purchased from the Cell Bank of the Chinese Academy of Sciences (Shanghai, China) and cultured in DMEM supplemented with 10% fetal bovine serum (FBS) at 37 °C in a humidified 5% CO_2 atmosphere.

2.3. *Animals*

Female Balb/c mice (18–20 g) were purchased from Beijing Vital River Experimental Animal Technology Co., Ltd., China. All animal handling and surgical procedures were conducted in strict accordance with the NIH Guidelines for the Care and use of Laboratory Animals. They were housed in standard laboratory conditions with free access to food pellets and drinking water. Anesthesia was performed by intraperitoneal injection with chloral hydrate.

2.4. *Design of breast mold and prosthesis preparation*

According to the different clinical implantations of the breast prosthesis (Fig. 2A), the interface and the bottom side of the mold were designed, including prosthesis section height *a*, the bottom radius b, the arc radius *r*, the length *c*, and the height *d*. For the designed prosthetic model, the model area S, the volume *V*, and the mass *m* of the prosthesis were calculated using the following formula by measuring the geometric data (Fig. 2B). The modeling parameters used in our study were as follows: $a = 4.8$ mm, $b = 5.6$ mm, $r = 5.66$ mm, ρ (the density of silicone rubber) $= 1.03$ g/cm^3, with the calculated results of $S = 170.62$ mm^2, $V = 35.08$ mm^3, $m = 1.9$ g. The CAD-designed prosthetic mold program was input into the photo-curing 3D printer (ANYCUBIC PHOTON-5.5, Zongheng Lifang Scientific Technology Co., Ltd., Shenzhen, China). The LCD resin was melted, extruded by the 3D printer at a high temperature, and rapidly solidified after molding (Fig. 2C). The PDMS and 1 ml of the silicone elastomer curing agent as the initiator were mixed thoroughly (100:5, w/w). The bubbles were removed under a vacuum, the mixture was poured into the above mold, and solidified for 55 min to obtain the mouse breast prosthesis.

2.5. *Safety of PDMS prosthesis*

To investigate the toxicity of a blank prosthesis on mice, a 3D printed blank prosthesis of PDMS was implanted surgically. Its effect on the heart, liver, spleen and lungs was evaluated using hematoxylin-eosin (H. E.) staining. The mouse's abdomen was depilated 24 h before the test with a hair removal area of 3 cm × 3 cm on the left and right sides of the midline. The abdominal skin was cut open, the PDMS prosthesis was implanted, and the wound was sutured; the implanted part was marked and photographed. After implantation, the animal's activities, feces, urine, eating and weight were observed. The mice were sacrificed on the 10th, 20th, and 30th d after implantation. The local and surrounding tissues, heart, liver, spleen, lung, and kidney were fixed in formalin, and H. E. pathological sections were prepared.

2.6. *Preparation of PTX, DOX microspheres and PPDM*

PTX is hydrophobic; therefore, PTX microspheres were prepared using the O/W single emulsion method [14]. In brief, PTX (10 mg) and PLGA (200 mg) were dissolved in dichloromethane (DCM, 2 ml) at 4 °C to prevent evaporation. This solution was added dropwise to 40 ml of a 2% (w/v) PVA aqueous solution, shaken at 3000 rpm for 2 min, and stirred continuously for 5 h at room temperature on a magnetic stirrer to evaporate DCM completely. The suspension was frozen and centrifuged at 1062.9 (× *g*) for 15 min. The supernatant was removed and the precipitate was washed with distilled water 3 times. After lyophilization for 24 h, the freeze-dried powder of microspheres was collected and stored in a desiccator until use.

DOX is a water-soluble drug and the W/O/W double emulsion method was used to prepare the DOX microspheres

[15]. DOX (10 mg) was dissolved in 20 ml of water and PLGA (200 mg) was dissolved in 2 ml of DCM at 4 °C. The solution of PLGA in DCM was added to the prepared DOX aqueous solution and emulsified at 3500 rpm to obtain the W/O emulsion. Then the W/O emulsion was added to 40 ml of the 2% PVA aqueous solution, stirred for 1 min at 3500 rpm, and stirred continuously for 5 h at room temperature to obtain the W/O/W multiple emulsion. The subsequent steps were the same as those for the PTX microspheres.

Prostheses loaded with free PTX and DOX (PPD) and PPDM were prepared according to the following steps. Briefly, PTX, DOX and microspheres of PTX and DOX were weighed and mixed with PDMS and its initiator (100:5, w/w). The mixture was mixed uniformly, vacuumed, degassed, and then poured into a mold coated with white petroleum jelly. Finally, they were solidified at 45 °C for 55 min, and demolded to obtain the prostheses for the mice's mammary gland.

2.7. Characterization of PPD and PPDM

The dynamic light scattering method was performed on a Zetasizer Nano ZS (Malvern, UK) to measure the size of the two microspheres. The microsphere suspension was diluted with water and measurements were taken at 25 °C. The zeta potential of the microspheres was also measured with the same instrument employed for the size measurements. The morphology of both of the microspheres and PPDM were observed using scanning electron microscopy (SEM; S-4800, HITACHI, Tokyo, Japan).

2.8. Measurement of drug loading efficiency and encapsulation efficiency

Contents of PTX and DOX in microspheres were determined using HPLC. PTX microspheres and DOX microspheres (10 mg) were dissolved in DCM (0.5 ml) and water (0.5 ml) and sonicated, respectively. Then, 2.5 ml of methanol was added, vortexed, and centrifuged at 800 rpm for 10 min to obtain the supernatant. The procedure was repeated for 3 times and all of the supernatants were analyzed using HPLC. HPLC experiments were conducted on an Agilent 1260 HPLC system (Santa Clara, CA, USA) with a DAD detector. The Diamonsil C_{18}–ODS HPLC column (4.6 mm × 250 mm, 5 μm) was purchased from Dikma Co., Ltd. (Beijing, China). The UV detector was set at 227 nm and 254 nm for PTX and DOX, respectively. The mobile phase for PTX measurement was methanol: water: acetonitrile = 40:25:35 (v/v) with a flow rate of 1 ml/min and an injection volume of 10 ml at 30 °C. The mobile phase for DOX measurement was sodium dodecylsulfate (2.88 mg/ml): acetonitrile: methanol = 500:500:60 (v/v) with a flow rate of 1 ml/min and an injection volume of 20 ml at 35 °C. Loading capacity and encapsulation efficiency were calculated according to the following equations:

Loading capacity (%) = (actual drug amount) / (weight of microspheres) × 100%

Encapsulation efficiency (%) = (actual drug amount) / (total drug amount) × 100%

2.9. Measurement of drug release from microspheres and prosthesis

PTX and DOX microspheres (5 mg) and one piece of PPDM were put into a beaker and then added with 10 ml of phosphate buffer (pH = 7.4), containing 0.1% (w/v) Tween 80 and 0.1% (w/v) Tween 20. After immediate shaking and mixing, the beaker was placed on a constant temperature oscillator at 200 rpm, 50 °C for 30 h. Samples (10 ml) were completely withdrawn for HPLC analysis and then quickly filled with the same amount of the release medium (32 °C) at 1, 3, 4, 7, 14, 21 and 30 h. The cumulative release (Q) was calculated according to the following equation.

$$Q = (C_n \times 50 + \sum C_n \times 2)/M \times 100\% \quad (1)$$

where, Q was the cumulative release ratio. C_n was the concentration of the sample n, C_i was the concentration of sample i, and M was the total drug amount.

The drug release mechanism was fitted using mathematical models, including zero order, first order, the Higuchi equation, and the Ritger-Peppas exponent equation. Equation fitting was calculated and the best model was identified as that with the highest correlation coefficient (r) [16].

2.10. In vitro cytotoxicity and synergic effect

The toxicity of single PTX or DOX, and their combinations, was measured using the cell counting kit-8 (CCK-8) assay. Briefly, 4T1-luc cells (3000 cells/well) were seeded into 96-well plates and cultured overnight. The cells were then incubated with media supplemented with single drugs or the drug combinations for 48 h. Cell viability was then measured according to the instructions of the CCK-8 assay. The dose-response curves were drawn according to the fractional cell inhibition against drug concentrations using the median effect model [17]. The combination index was calculated according to the dose-response curves [18].

2.11. Cellular uptake of DOX microspheres

The cellular uptake behavior of DOX microspheres was determined by confocal laser scanning microscopy (CLSM) using 4T1-luc cells. The cells were seeded on coverslips in 6-well plates at a density of 2.5×10^5 cells per well in 2 ml of DMEM and cultured for different times, and then the original medium was replaced with free DOX and DOX microspheres (DOX-equivalent concentration of 500 nM), which were incubated with the cells for 12, 24 and 48 h. At each time point, the slides were taken out for fixation, staining and sealing. The cells were washed 3 times with phosphate-buffered saline (PBS), fixed with 4% paraformaldehyde for 20 min, and washed a further 3 times with PBS. The cells were finally stained with DAPI for 20–30 min (DAPI stock solution was diluted 100 times with PBS), and washed 3 imes with PBS (Being careful not to drop the PBS directly onto the slide to avoid crushing

the cells). The cell nuclei were stained with DAPI according to the standard protocol provided by the supplier. The coverslips were placed onto the glass microscope slides. The subcellular localization and intracellular DOX release of microspheres were visualized under a laser scanning confocal microscope.

2.12. *Pharmacodynamic study*

Female Balb/C mice (18–20 g) were purchased from the Vital River Experimental Animal Technology Co. Ltd. (Beijing, China). The animals were maintained in the animal laboratory under specific pathogen free (SPF) conditions. 4T1-luc cells (1×10^7 cells/ml, 0.1 ml) were inoculated subcutaneously into the right flank of each mouse to observe tumor growth. When the tumor volume reached approximately 100 mm^3, the mice with tumors were imaged using a non-invasive fluorescence imaging system (IVIS Spectrum, Perkin Elmer, Waltham, MA, USA) to ascertain the successful establishment of the tumor model. The mice were randomly divided into 5 groups ($n = 7$). The tumor was resected completely by surgery and this day was designated as Day 0. Each mouse is injected intraperitoneally with penicillin sodium solution (4 IU, 0.5 ml) for 3 d The mice were treated with the different medical treatments as follows. The tumor-bearing mice in Group I (Model) were injected with saline. The mice in Group II (Injection) were injected with DOX & PTX injection intraperitoneally, with a PTX dose of 38 mg/kg and a DOX dose of 12.5 mg/kg on day 0, 7, and 14. The mice in Group III (Control) were implanted with a blank prosthesis subcutaneously. The mice in Group IV (PPD) were implanted with a prosthesis of PTX and DOX (PPD) subcutaneously with a PTX dose of 38 mg/kg and a DOX dose of 12.5 mg/kg. The mice in Group V (PPDM) were implanted with PPDM subcutaneously with a PTX dose of 38 mg/kg and a DOX dose of 12.5 mg/kg.

Mice were weighed every other day from the first day of surgical resection and the weight changes were recorded. Recurrence and transformation of luciferous tumors in mice were observed using non-invasive fluorescence imaging on day 14 and 21. Mice were depilated before imaging and were kept anesthetized under continuous isoflurane flow. Autofluorescence and undesired background signals were eliminated by spectral analysis using a blank control mouse without tumors as the background. The mice were then sacrificed, and the tumor, heart, liver, spleen and lungs were taken out and fixed in 10% formaldehyde solution. H.E.-stained histopathological slides were prepared according to the standard protocol and observed under an inverted fluorescence microscope (BDS200-FL, Chongqing Optec Instrument Co., Ltd, Chongqing, China). Immunohistochemical detection of CD31 expression in tumors and lungs was performed as previously reported [19]. The obtained slides were observed using the BDS200-FL microscope and analyzed using Image-Pro-Plus 6.0 software (Media Cybernetics, Rockville, MD, USA. In addition, inhibition by PPDM of tumor cell apoptosis was investigated by terminal deoxynulceotidyl transferase nick-end-labeling (TUNEL) staining.

2.13. *Statistical analysis*

All experiments were repeated three times and expressed as means ± standard deviations (SD). Statistical significances were analyzed using SPSS19.0 software (IBM Corp., Armonk, NY, USA. One way analysis of variance (ANOVA) with a post-hoc Tukey's test was employed to identify significant differences ($P < 0.05$ or $P < 0.01$) between data sets.

3. Results and discussion

3.1. *Characteristics of PTX & DOX microspheres*

Solvent evaporation is an important method to prepare microspheres for drug delivery [14]. The parameters of the preparation process affected the particle size and morphology of the microspheres, such as ultrasonic time, power, solvent evaporation time and stirring rate. Insufficient ultrasonic time leads to insufficient emulsification of the microspheres and a low microsphere yield. High ultrasonic power makes the microspheres small, which causes relatively quick drug release from the microspheres. The stirring rate also affected the morphology of the microspheres. A faster stirring rate could break the microspheres into pieces and destroy their perfect morphology. Both the PTX and DOX microspheres were completely round, with an average particle size of 3.1 and 2.2 μm, respectively (Fig. 3A). The encapsulation efficiency of the PTX microspheres and DOX microspheres were 84% ± 4.6% and 70% ± 4.6% with particle sizes of 4.1 ± 3.1, 4.0 ± 2.2 μm and the zeta potential of −16.2 ± 0.3, −16.5 ± 0.1 mV, respectively.

Biodegradable sustained release microspheres can release drugs at a certain rate over several weeks or months to maintain an effective concentration and reduce the frequency of drug administration; however, the period of sustained release from microspheres *in vitro* is long, which causes difficulties for prescription screening and daily quality control. An accelerated release test can solve this problem [20,21]. The microspheres could release PTX or DOX continuously for up to 30 h (Fig. 3B), and the concentration at different time points all reach the 80% inhibitory concentration for PTX of 733 nM and DOX of 948 nM on 4T1-luc cells (unpublished data). A suitable *in vitro* release test method can better reflect the release correlation of microspheres *in vivo*, which is beneficial to identify ideal prescriptions and processes. The release profile of the microspheres obviously affects treatment efficacy. However, the commonly used *in vitro* release assay of the sustained-release microspheres usually takes a long time, which is a challenge for optimization and quality control. The accelerated release test can better solve the problem [22]. Surprisingly, we found that the release method had an important effect on the amount release and the release rate from the microspheres. There was almost no drug release using the dialysis bag, but the release behavior was good using the glass beaker. There might be a strong adsorption between the dialysis bag and the microspheres, resulting in little drug release.

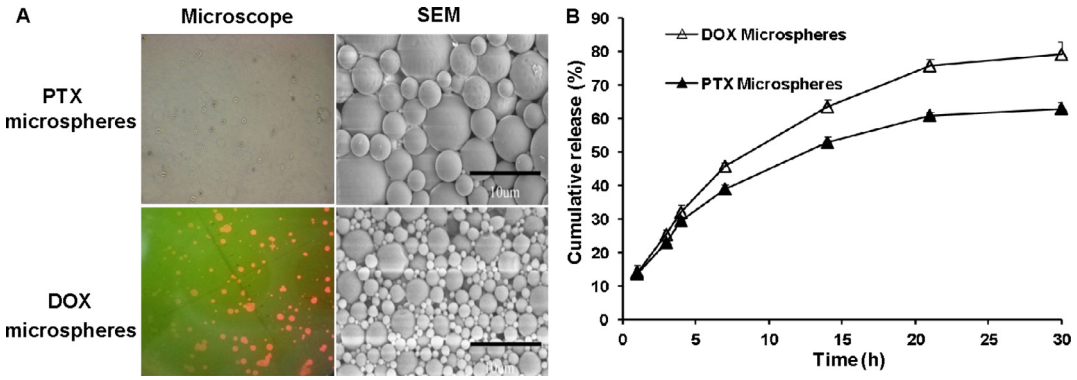

Fig. 3 – Morphology (A) and the cumulative *in vitro* release (B) of PTX and DOX microspheres.

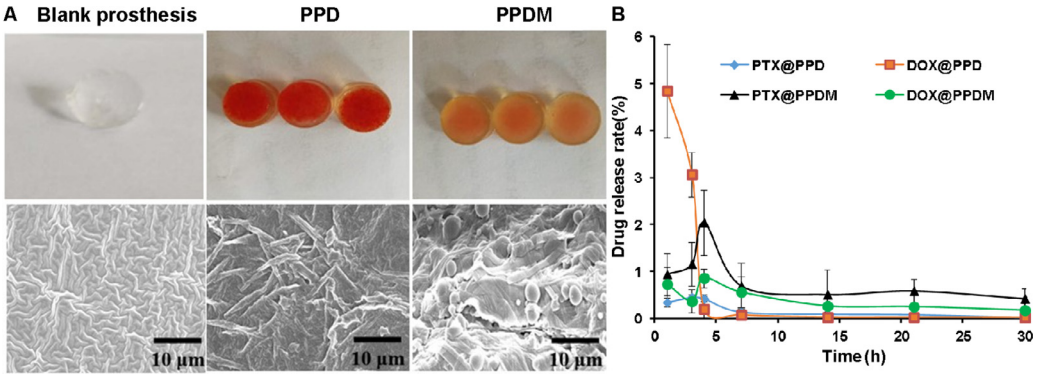

Fig. 4 – Morphology and *in vitro* drug release of the prosthesis. (A) Morphology and inner structure of blank prosthesis, PPD and PPDM. (B) The cumulative release of PTX and DOX from a PPD and PPDM, respectively. The scale bars indicate 10 μm.

3.2. *Characteristics of PPDM*

The preparation process of PPD or PPDM via the perfusion method involves various preparation parameters, such as the mixing degree of drugs with the PPDM matrix, the ratio of the curing agent, the curing time, and temperature. If the curing time was too long, it affected the drug's stability and reduced the drug loading efficiency. By contrast, insufficient curing time resulted in failure of the formation of the prosthesis. The PPDM still maintained their spherical morphology, as observed by SEM. This indicated that microspheres and blank prosthesis were only mixed by physical interaction (Fig. 4A).

Based on 3D printing technology [23], PPDM were prepared to inhibit tumor recurrence and metastasis after breast conserving surgery, with the simultaneous function of breast reconstruction. Personal customization with 3D printing technology ensured that the silicone prosthesis could be matched perfectly with the lesion based on the anatomical features of the patient's mastectomy site. The sustained release of the microspheres could ensure precise and continuous medical treatment.The drug release results showed that PPDM could release PTX and DOX continuously and simultaneously within 30 h. The sustained release profiles demonstrated no sudden release at the initial stage. For the release behavior of DOX (Fig. 4B), the cumulative release rate of DOX in PPD was 4.8%, which showed a significant burst release behavior, because DOX is a drug with good water solubility. The dissolution rate is very fast, and a sudden release effect occurs. DOX release suddenly decreased to 3% at 3 h, and the cumulative release rate at 5 h was 0.2%. The release rate at subsequent times was close to zero. Therefore, even if the local drug concentration is higher at 1 h, with the progress of the body's metabolic processes, free DOX is easily metabolized, and the drug effect cannot be maintained, let alone the exertion of synergy. The release of DOX from PPDM showed no obvious sudden release behavior at 1 h, and the drug was released at a relatively constant rate from 2 h. We speculated that a more stable pore channel had been formed at this time, allowing smooth drug release. The released amounts reached the 80% inhibition concentration for PTX of 733 nM and DOX of 948 nM, based on our unpublished data, indicating that the PPDM might inhibit tumor cell growth or migration. The release profile best matched the Higuchi equation (Table 1). This was advantageous for a continuous and effective effect on tumor inhibition. Therefore, while maintaining an effective drug concentration, it is also beneficial for DOX to exert its synergistic effect with PTX and improve tumor cell killing. We analyzed the causes of two different release phenomena. Matrix erosion, including PLGA and PDMS, played an important role in drug release [24]. First, the water-soluble drug DOX was wrapped in the polymer material PLGA. The PLGA microspheres have a more obvious slow-release effect than the free drug, effectively avoiding its sudden release. This is consistent with the above microsphere

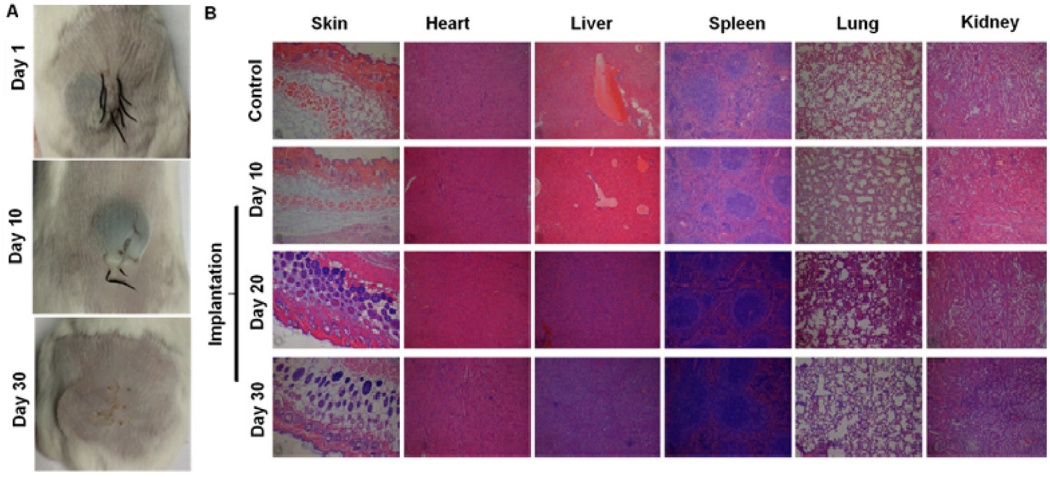

Fig. 5 – (A) Healing of the back suture on the 10th and 30th d after prosthesis implantation. (B) Pathological changes of the major tissues on the 10th, 20th and 30th d after prosthesis implantation (100 ×).

Table 1 – *In vitro* release simulation of PTX and DOX from PPDM.

Drug Release	Simulation model	Equation	r
PTX	Zero order	$Q_n = 0.3202t + 2.7693$	0.88
	First order	$\ln(100\text{-}Q_n) = -0.037t + 4.5761$	0.85
	Higuchi	$Q_n = 2.19t^{1/2} + 0.209$	0.95
	Ritger-Peppas	$\ln Q_n = 0.789\ln t + 0.29$	0.77
DOX	Zero order	$Q_n = 0.0955t + 0.9985$	0.78
	First order	$\ln(100\text{-}Qn) = -0.0013t + 4.5916$	0.83
	Higuchi	$Qn = 6.75t1/2 + 0.441$	0.90
	Ritger-Peppas	$\ln Qn = 0.767\ln t + 0.97$	0.86

release curve. Similarly, we could not ignore the delayed effect of PDMS on drug release. For the release of PTX, release from the PPD was relatively stable at 1—4 h, and after 4 h, the drug release rate was significantly reduced, with a value approaching 0.1%, and the amount of drug released was too small. In this way, the concentration of local antitumor drugs cannot be guaranteed; however, the release of PTX from the PPDM was relatively gentle. Its minimum cumulative release rate was 0.5%, and it is sufficient to exert an 80% inhibitory anticancer effect; therefore, the drug could be maintained at an effective concentration, and can play a synergistic effect with DOX released at the same time. The evaluation of the synergy was based on our unpublished data. It demonstrated that the 3D-printed prosthesis loaded with microspheres of PTX and DOX could release the drugs continuously for more than 3 weeks and thereby suppress cancer recurrence with reduced side effects.

To evaluate the safety of PDMS, PPDM were implanted subcutaneously and the topical irritation was observed (Fig. 5A). The diets, weight, activity, and routine habits of the mice were similar to the mice in the control group within 30 d after prosthesis implantation. There was no redness and fever in the local area after prosthesis implantation, and the surgical incision healed quickly and well. H.E. staining (Fig. 5B) showed no obvious pathological changes of the mouse epidermis, there was only mild inflammatory cell infiltration on Day 1. There was slight thickening inflammation of the alveolar wall; however, this situation was restored to normal on Day 20. By 30 d, the inflammation had disappeared. Overall, there was no significant toxicity or topical irritation.

3.3. *In vitro cytotoxicity of PTX and DOX and the combination index*

Combination chemotherapy is widely applied clinically to enhance therapeutic efficacy and alleviate side effects [25]. PTX and DOX possess different anticancer mechanisms and are used for the combination treatment of cancers, demonstrating a synergistic effect [26]. Both PTX and DOX alone markedly inhibited the proliferation of 4T1 cells, with IC_{50} values of 261.3 nM and 331.3 nM, respectively. Furthermore, the PTX microspheres and DOX microspheres had better anticancer effects than the free drugs, with lower IC_{50} values of 197.5 nM and 243.9 nM, respectively. The combination indexes (CI, <1) of the two drugs (10:3 combination) further confirmed their synergistic effect (Fig. 6).

3.4. *Cellular uptake of DOX microspheres*

The results of phagocytosis assays showed that free DOX and DOX microspheres entered 4T1-luc cells. The red fluorescence appeared in both groups at 24 h; DOX fluorescence was significantly enhanced at 48 h, and the fluorescence intensity of DOX microspheres was further enhanced. The fluorescence intensity of the DOX microspheres was larger than of the free DOX group, and the nuclear atrophy of the microsphere group was more obvious, indicating that the cells had undergone apoptosis. The DOX microspheres had a stronger effect within 48 h (Fig. 6E).

3.5. *Highly efficient prevention of breast cancer recurrence by PPDM*

Currently, the majority of invasive and noninvasive breast cancers are treated by breast conservation therapy (BCT),

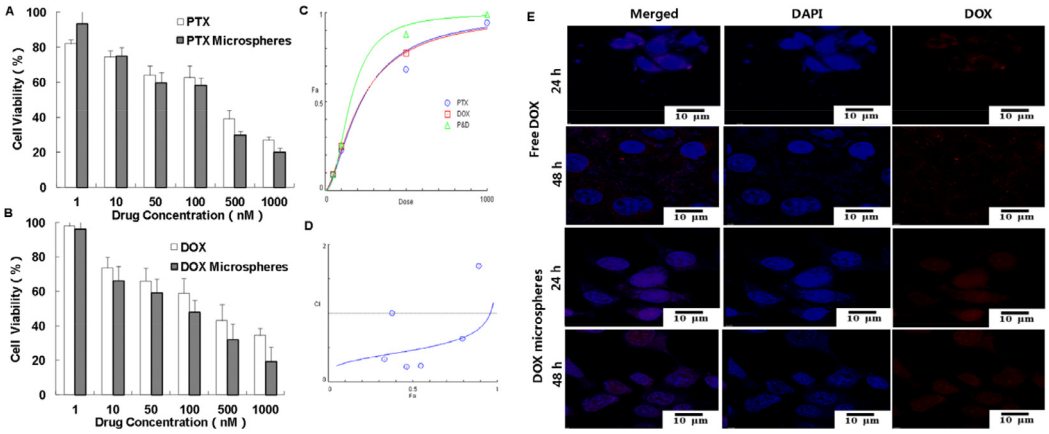

Fig. 6 – (A) *In vitro* cytotoxicity of free PTX and PTX microspheres on 4T1–luc cells. (B) *In vitro* cytotoxicity of free DOX and DOX microspheres on 4T1–luc cells. (C) The dose-effect profile of combination of PTX and DOX. (D) The effect-index profile of combination of PTX and DOX. (E) Cellular uptake of free DOX and DOX microspheres by 4T1-luc cells.

which includes wide local excision and subsequent radiation treatment. Nevertheless, the incidence of local-regional recurrence and distant metastases after BCT is common, which correlates positively with the grade of malignancy [27]. In the present study, Balb/c mice were used to establish a breast cancer model with local recurrence and metastasis. *In vivo* imaging techniques were used to characterize whether the model was successfully established and the subsequent pharmacodynamics effect. The fluorescence intensity of the mice with breast cancer tumors was relatively strong before surgical excision. Then, the mice were grouped randomly, the tumors were excised, and there was no fluorescence signal in the tumor resection sites, which indicated that there was no residual tumor or metastasis elsewhere.

On the 14th d after incision, the previous tumor sites showed different fluorescence signal intensities, indicating local recurrence. The order of fluorescence intensities was as follows: Group I (Model) > Group III (Control) > Group IV (PPD) > Group II (Injection) > Group V (PPDM). At this time point, there was no lung metastasis in any of the groups. The inhibitory effect of PPDM was the most obvious and was equivalent to that of Group II (Injection). On the 21st d post-surgery, the fluorescence signal intensity of each group became stronger. In addition, the model group, the blank prosthesis group, and Group IV (PPD) mice showed more obvious tumor metastasis (Fig. 7A). Local-regional recurrence or distant metastatic growth in the lungs is caused by the presence of disseminated or circulating tumor cells [28]. Despite some medical progress, there has been no significant improvement in the treatment of postoperative recurrence and metastasis. In view of the many anti-tumor advantages of local chemotherapy, clinicians have used direct intra-tumor delivery of chemotherapy drugs extensively to increase local efficacy. However, when drugs are directly injected into the tumor, they are easily cleared at the administration site. Therefore, an effective formulation to deliver chemotherapy drugs into tumors with a sustained release effect is required, which can be implanted or injected in peritumoral sites after tumor resection to achieve local long-term chemotherapy [4].

According to different pathogenetic conditions, there have been diverse applications of chemotherapy drugs. Local sustained-release chemotherapy can also be implanted before surgery to control the primary tumor, such that the tumor shrinks to reduce the scope of surgical resection [29,30]. Postoperative implants can used as adjuvant chemotherapy to kill residual tumors or subclinical lesions. In patients with advanced or metastatic tumors, systemic chemotherapy can be performed at the same time with local sustained-release implantation around a solid tumor with high drug loading, which can result in a concentrated attack on the tumor [31]. PTX and DOX were the first class of combined chemotherapeutic drugs used to treat breast cancer [32]. A controlled and sustainable release of PTX and DOX can induce continuous apoptosis of tumor cells by stopping microtubule disassembly, thereby preventing cell division [33,34]. In the present study, the inhibitory effect of PPDM on tumor recurrence was better than that in the other groups, and was equivalent to that of Group II (Injection) (Fig. 7B). However, the mortality of the mice in Group II (Injection) was higher than that in the PPDM group, indicating that PPDM maintained a local effective therapeutic concentration and had a synergistic effect.

Lung metastasis is an important index to evaluate the chemotherapeutic effect after incision. There were obvious fluorescence signals in the lungs of the mice in the model, blank prosthesis, and Group IV (PPD), which indicated that lung metastasis had occurred. In addition, some pulmonary nodules also appeared in the lungs of the mice in the model, the blank prosthesis, and the PPD groups (Fig. 7C). The results further illustrated the local recurrence and metastasis of breast cancer. PPDM (Group V) showed a better inhibitory effect than that of the model and the blank prosthesis groups on recurrence and metastasis in mice (Fig. 7D). In comparison, one mouse died in Group II (Injection), possibly because of the toxicity of PTX and DOX delivered via direct intraperitoneal injection.

PTX is a broad-spectrum anticancer drug with a unique anti-microtubule mechanism [35]. It promotes the assembly of tubulin dimers into microtubules, prevents its

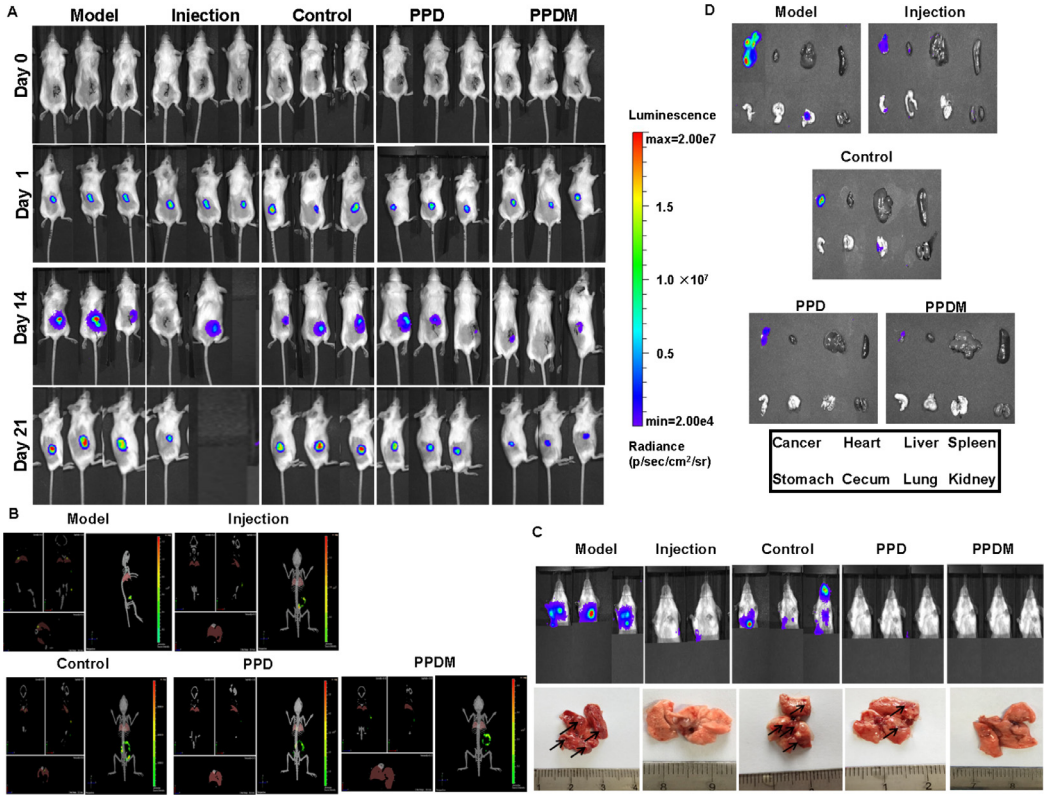

Fig. 7 – PPDM inhibited the recurrence and metastasis of breast cancer in mice after ablation. Representative bioluminescent images of mice in the different groups in the 2D mode (A) and 3D mode (B). (C) Lung metastasis of mice in the different groups. (D) Fluorescence of the major organs.

depolymerization and stabilizes microtubules, which allows cancer cells to be fixed in the mitosis process, eventually resulting in their death. However, it cannot affect the synthesis of DNA, RNA and proteins [36]. In comparison, DOX interferes with DNA transcription and can bind to the corresponding proteins, thereby inhibiting the synthesis of intracellular RNA, protein and DNA, which kills cancer cells. Combination chemotherapy with PTX and DOX is a first-line clinical treatment protocol [37]. Its superiority is mainly manifested in the following aspects [38]: (1) Chemotherapy drugs with different anti-tumor mechanisms would produce synergistic effects in killing tumor cells [39]; (2) single chemotherapeutic drugs are commonly delivered as a large dose and with a long treatment time, which leads to marked levels of side effects in patients. Combination chemotherapy could eliminate this possibility using several different chemotherapeutic drugs. Therefore, combination chemotherapy is important to treat cancer by improving the synergistic effect and reducing systemic side effects. In the present study, there was no significant metastasis in Group V (PPDM) because of the simultaneous release of PTX and DOX.

Assessment of *in vivo* toxicity via mouse body weight evaluation was performed on all the animal groups during the 21 days after prosthesis implantation. No signs of *in vivo* toxicity or other physiological complications were observed in any of the animals during this period, as indicated by the preservation of steady body weight, which suggested that the prosthesis was biocompatible (Fig. 8A) [40]. Finally, we calculated the tumor recurrence rate among the groups (Fig. 8B), which was also consistent with the living image results.

3.6. *Histopathological changes and tumor metastasis*

On the 21st d after incision, the major tissues, including the heart, liver, spleen, lung and kidney, were dissected. H.E. staining was performed to observe the pathological changes, which showed that the lungs had different numbers of lesions in the mice of the model, blank prosthesis and Group IV (PPD). In addition, the lung metastases of the mice in Group I (Model), Group II (Injection) and Group IV (PPD) lost their normal structure to different extents. The alveolar cavity was solidified and showed solid deformation, which was caused by the presence of tumor nodules. The mice in the model group and the blank prosthesis group showed the most obvious metastasis, and there were no obvious lesions in the mice of PPDM group (Fig. 9A). CD31 is an angiogenic marker, and its increased level indicates active tumor growth. Immunohistochemistry showed that the model group had the most obvious positive expression of CD31 *in situ* breast cancer. The Group II (Injection) and Group V (PPDM) had the least staining for CD31 (Fig. 9B). Similar results were obtained for lung metastasis. PPDM also demonstrated the most significant apoptosis of tumor cells, which was similar

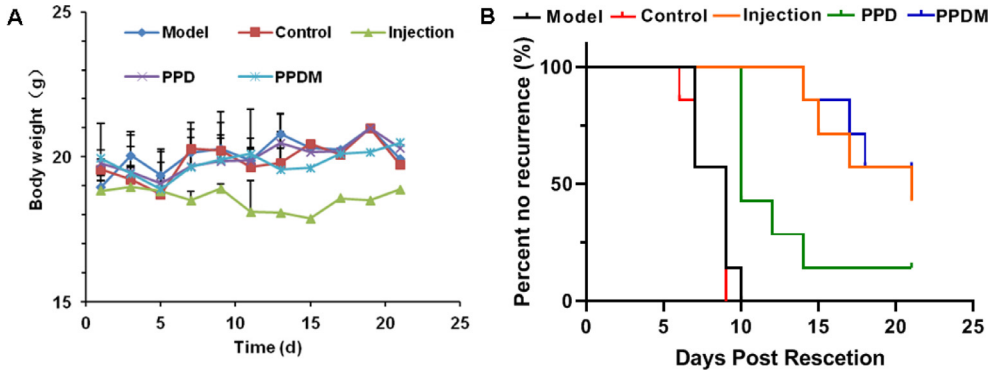

Fig. 8 – (A) The weight changes among the different groups. (B) Incidence of breast cancer recurrence among the different groups of mice.

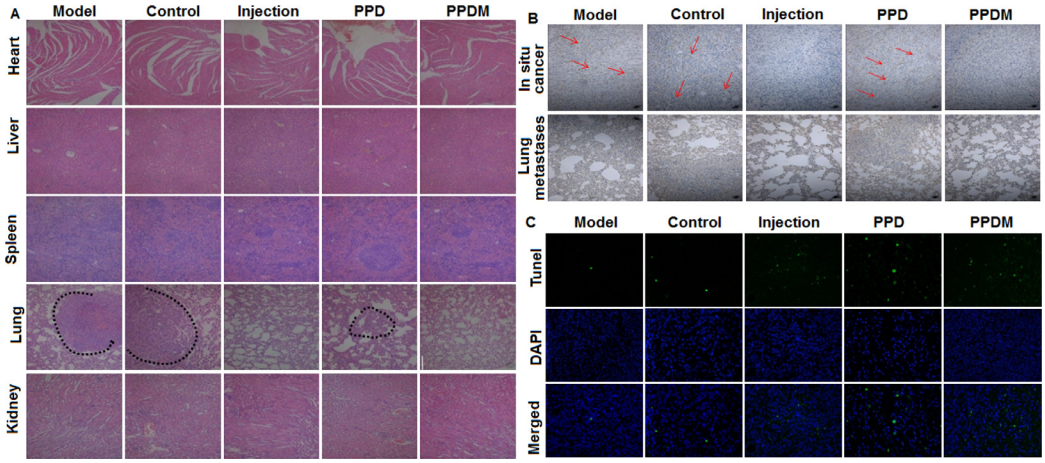

Fig. 9 – Inhibitory effect of PPDM on the recurrence and metastasis of breast cancer in mice. (A) H.E. (hematoxylin and eosin) histopathological staining of major tissues in different groups. (B) PPDM suppressed the expression of CD31 and inhibited breast cancer metastasis to lung. (C) PPDM promoted the apoptosis of cancer cells in the lung *in vivo*.

to that of Group II (Injection), and better than that of Group I (Model), Group III (Control) and Group IV(PPD) (Fig. 9C). This might be related to the continuous cytotoxic action of PTX and DOX.

4. Conclusions

The PPDM showed good biocompatibility and obvious inhibitory effects on the local recurrence and metastasis of breast cancer in mice. The combined use of PTX and DOX had a synergistic effect, a long-acting duration time, and low toxicity. PPDM are expected to provide a promising choice for simultaneous breast reconstruction and breast cancer treatment after breast conserving surgery.

Conflicts of interest

The authors report no conflicts of interest. The authors alone are responsible for the content and writing of this article.

Aknowledgement

We thank the National Natural Science Foundation of China (No. 81472951) for financial support of this work.

REFERENCES

[1] Fan L, Strasser Weippl K, Li J. Breast cancer in China. Lancet Oncol 2014;15(7):e279–89.
[2] Siegel R, Miller K, Jemal A. Cancer statistic. CA Cancer J Clin 2018;68(1):7–30.
[3] Gerow FJ, Spira M, Hrady S. Plastic surgery applications of synthetic implants. Med Instru 1973;7(2):96–9.
[4] Lundberg BB, Resovie V, Ramaswamy M, Wasan KM. A lipophilic paclitaxel derivative incoporated in a lipid emulsion for parenteral administration. J Control Release 2003;86(1):93–100.
[5] Goyanes A, Usanee DA, Wang J. 3D scanning and 3D printing as innovative technologies for fabricating personalized topical drug delivery systems. J Control Release 2016;234:41–8.

[6] Fu J, Yu X, Jin Y. 3D printing of vaginal rings with personalized shapes for controlled release of progesterone. Int. J. Pharm 2018;539:75–82.
[7] Patel BR, Solorio L, Wu HP, Krupka T, Exner AA. Effect of injection site on *in situ* implant formation and drug release *in vivo*. J Control Release 2010;147(3):350–8.
[8] Zeng Q, Zhu YW, Yu BR, Sun YJ, Ding XK, Xu C, et al. Antimicrobial and antifouling polymeric agents for surface functionalization of medical implants. Biomacromol 2018;19(7):2805–11.
[9] Wu BM, Borland SW, Giordano RA, Cima LG, Sachs EM, Cima MJ. Solid free-form fabrication of drug delivery devices. J Control Release 1996;40(1–2):77–87.
[10] Santos TC, Rescignano N, Boff L, Reginatto FH, Simões CMO, de Campos AM, et al. Manufacture and characterization of chitosan/PLGA nanoparticlesnanocomposite buccal films. Carbohydr Polym 2017;173:638–44.
[11] Matthes K, Mino-Kenudson M, Sahani DV, Holalkere N, Fowers KD, Rathi WR. EUS-guided injection of paclitaxel (OncoGel) provides therapeutic drug concentrations in the porcine pancreas (with video). Gastrointest Endosc 2007;65(3):448–53.
[12] Jassem J, Pienkowski T, Pluzanska A, Jelic S, Gorbunova V, Berzins J. Doxorubicin and paclitaxel *versus* fluorouracil, doxorubicin and cyclophosphamide as first-line therapy for women with ad vanced breast cancer: long-term analysis of the previously published trial. Onkologie 2009;32(8–9):468–72.
[13] Rajendra P, Aiiella S, Boris V, Domb AJ. Intravenous and regional paclitaxel formulations. Curr Med Chem 2004;11:397–402.
[14] Wada R, Hyon SH, Ikada Y. Lactic acid oligomer microspheres containing hydrophilic drugs. J Pharm Sci 2010;79(10):919–24.
[15] Ruan G, Feng SS. Preparation and characterization of poly(lactic acid)–poly(ethylene glycol)–poly(lactic acid) (PLA–PEG–PLA) microspheres for controlled release of paclitaxel. Biomaterials 2003;24(27):5037–44.
[16] Mohanty C, Sahoo SK. The *in vitro* stability and *in vivo* pharmacokinetics of curcumin prepared as aqueous nanoparticulate formulation. Biomaterials 2010;31(25):6579–611.
[17] Vogus DR, Evans MA, Pusuluri A, Barajas A, Zhang MW, Krishnan V, et al. A hyaluronic acid conjugate engineered to synergistically and sequentially deliver gemcitabine and doxorubicin to treat triple negative breast cancer. J Control Release 2017;267:191–202.
[18] Chou T. Drug combination studies and their synergy quantification using the Chou-Talalay method. Cancer Res 2010;70:440–6.
[19] Avramis IA, Kwock R, Avramis VI. Taxotere and vincristine inhibit the secretion of the angiogenesis inducing vascular endothelial growth factor (VEGF) by wild-type and drug-resistant human leukemia T-cell lines. Anticaner Res 2001;21(4A):2281–6.
[20] Alexis F. Factors affecting the degradation and drug-release mechanism of poly(lactic acid) and poly[(lactic acid)-co-(glycolic acid)]. Polym Int 2005;54:36–46.
[21] Raval A, Bahadur P, Raval A. Effect of nonionic surfactants in release media on accelerated *in-vitro* release profile of sirolimus eluting stents with biodegradable polymeric coating. J Pharm Anal 2018;8:45–54.
[22] Xu Q, Chin SE, Wang CH, Pack DW. Mechanism of drug release from double-walled PDLLA(PLGA) microspheres. Biomaterials 2013;34(15):3902–11.
[23] Vaishnavi K, Dhananjay B, Kishore P. Assessment of an integrative anticancer treatment using an *in vitro* perfusion-enabled 3D breast tumor model. Biomaterials 2018;4(4):1407–17.
[24] Mi F, Shyu S, Lin Y, Wu Y, Peng C, Tsai Y. Chitin/PLGA blend microspheres as a biodegradeble drug delivery system:a new drug delivery system of protein. Biomaterials 2003;24(1):5023–36.
[25] Shen W, Chen X, Luan J, Wang D, Yu L, Ding J. Sustained codelivery of cisplatin and paclitaxel via an injectable prodrug hydrogel for ovarian cancer treatment. ACS Appl Mater Interf 2017;9:40031–46.
[26] Jean M, Joseph G. The role of taxanes in the treatment of breast cancer. Expe Opin Phar 2005;6(7):1073–94.
[27] Huston TL, Simmons RM. Locally recurrent breast cancer after conservation therapy. Am J Surg 2005;189(2):229–35.
[28] Bidard FC, Salomon AV, Gomme S, Nos C, de Rycke Y, Thiery JP. Disseminated tumor cells of breast cancer patients: a strong prognostic factor for distant and local relapse. Clin Cancer Res 2008;14(11):3306–11.
[29] Krukiewicz K, Zak JK. Biomaterial-based regional chemotherapy: local anticancer drug delivery to enhance chemotherapy and minimize its side-effects. Mater Sci Eng C 2016;62:927–42.
[30] Indolfi L, Ligorio M, Ting DT, Xega K, Tzafriri AR, Bersani F. A tunable delivery platform to provide local chemotherapy for pancreatic ductal adenocarcinoma. Biomaterials 2016;93:71–82.
[31] Chew SA, Danti S. Biomaterial-based implantable devices for cancer therapy. Adv Healthc Mater 2017;6:160–6.
[32] Hemda BC, Laura IV, Harald RK, boock AE, Yeini E. *In vivo* comparative study of distinct polymeric architectures bearing a combination of paclitaxel and doxorubicin at a synergistic ratio. J Control Release 2017;257:118–31.
[33] Horwitz S. Mechanism of action of taxol. Trends Pharma Sci 1992;13:134–5.
[34] Minotti G, Anthracylines Menna P. molecular advances and pharmacologic developments in antitumor activity and cardiotoxity. Pharmacol Rev 2004;56(2):185–229.
[35] Taxol Arbuck SG. (paclitaxel): future directions. Ann Oncol 1994;5(6):S59–62.
[36] Safavy A, Bonner JA, Waksal HW, BuchsbaumDJ Gillespie GY, Khazaeli MB. Synthesis and biological evaluation of paclitaxel-C225 conjugate as model for targeted drug delivery. Bioconjug Chem 2003;14(2):302–10.
[37] Blanco E, Ferrari M. Emerging nanotherapeutic strategies in breast cancer. Breast 2014;23(1):10–18.
[38] Wang Y, Ma S, Xie Z, Haishan Z. A synergistic combination therapy with paclitaxel and doxorubicin loaded micellar nanoparticles. Colloids Surf B Biointerf 2014;116:41–8.
[39] Zhang T, Chen Y, Li J, Yang FF, Wu HG, Dai FJ. Antitumor action of a novel histone deacetylase inhibitor, YF479, in breast cancer. Neoplasia 2014;16(8):665–77.
[40] Conde J, Oliva N, Zhang Y, Artzi N. Local triple-combination therapy results in tumour regression and prevents recurrence in a colon cancer model. Nat Mater 2016;15:1128–39.